Asymmetric W-shaped and M-shaped soliton pulse generated from a weak modulation in an exponential dispersion decreasing fiber*

Xiang-Shu Liu(刘祥树)[1,2], Li-Chen Zhao(赵立臣)[1,3], Liang Duan(段亮)[1,3], Zhan-Ying Yang(杨战营)[1,3,†], and Wen-Li Yang(杨文力)[3,4]

[1] School of Physics, Northwest University, Xi'an 710069, China
[2] Faculty of Science, Qinzhou University, Qinzhou 535000, China
[3] Shaanxi Key Laboratory for Theoretical Physics Frontiers, Xi'an 710069, China
[4] Institute of Modern Physics, Northwest University, Xi'an 710069, China

(Received 25 July 2017; revised manuscript received 17 August 2017; published online October 20 2017)

We study localized waves on continuous wave background in an exponential dispersion decreasing fiber with two orthogonal polarization states. We demonstrate that asymmetric W-shaped and M-shaped soliton pulse can be generated from a weak modulation on continuous wave background. The numerical simulation results indicate that the generated asymmetric soliton pulses are robust against small noise or perturbation. In particular, the asymmetric degree of the asymmetric soliton pulse can be effectively controlled by changing the relative frequency of the two components. This character can be used to generate other nonlinear localized waves, such as dark–antidark and antidark–dark soliton pulse pair, symmetric W-shaped and M-shaped soliton pulse. Furthermore, we find that the asymmetric soliton pulse possesses an asymmetric discontinuous spectrum.

Keywords: asymmetric soliton pulse, asymmetric discontinuous spectrum, exponential dispersion decreasing fiber

PACS: 05.45.Yv, 42.65.Tg, 42.81.Dp **DOI:** 10.1088/1674-1056/26/12/120503

1. Introduction

Optical localized waves have recently become a topic of intense research in nonlinear fiber system, such as bright soliton, dark soliton, breather, and rogue wave.[1–8] Considering the modes are usually more than 1, many studies have been done to find out if there are some new excitation properties in coupled systems. Explicitly, it is found that there are much more abundant localized waves in coupled systems, such as vector solitons,[9–12] vector rogue waves,[13–17] and vector breathers.[13,14,18] These vector localized waves demonstrate many dynamics properties different from the scalar ones. However, most of them admit symmetric profile in temporal distribution. We would like to find if there can be some asymmetric solitons in nonlinear fiber systems.

On the other hand, a soliton is usually obtained from localized pulses.[19] Recent studies suggested that it is possible to obtain rogue waves from weak modulations on continuous wave background (CWB).[20,21] If we can find some ways to stabilize the rogue wave signals, then it is possible to obtain soliton pulse from weak modulations on CWB. Moreover, modulational instability (MI) plays an important role in the dynamics of a nonlinear localized wave.[22] These characters have been used to obtain the soliton in the exponential dispersion decreasing fiber with one component.[23,24] Considering the MI character in coupled systems is different from the ones in uncoupled systems, we expect that there are some different dynamical processes in an exponential dispersion decreasing fiber with two orthogonally polarized states.

In this paper, we study nonlinear excitation in an exponential dispersion decreasing fiber with two orthogonal polarization states. We demonstrate asymmetric W-shaped and M-shaped soliton pulses are generated from a weak modulation on CWB in the fiber, in contrast to symmetric ones obtained before. The numerical results indicate that the generated asymmetric soliton pulses are robust against small noise or perturbation. The dynamical process is explained by qualitatively based MI analysis, which evolves from MI regime to modulational stability (MS) regime. In particular, the asymmetric degree of the asymmetric soliton pulse can be controlled effectively by changing the relative frequency of two components, which is used to generate other type soliton pulses. Furthermore, spectral analysis is carried out on the asymmetric soliton pulse. It is shown that the spectrum is asymmetric and discontinuous. The results provide a possible way to obtain asymmetric soliton pulses from weak modulations, which is different from previous methods.

The paper is organized as follows. In Section 2, we describe the physical model of an exponential dispersion decreasing fiber and present analytic solution, which can be used to describe the evolution of a weak disturbance on continu-

*Project supported by the National Natural Science Foundation of China (Grant No. 11475135), the Fund from Shaanxi Province Science Association of Colleges and Universities (Grant No. 20160216), and Guangxi Provincial Education Department Research Project, China (Grant No. 2017KY0776).

†Corresponding author. E-mail: zyyang@nwu.edu.cn

© 2017 Chinese Physical Society and IOP Publishing Ltd

ous wave backgrounds. In Section 3, we present the dynamic process of asymmetric soliton pulse generated from a weak modulation in the exponential dispersion decreasing fiber. We show that the asymmetric degree of soliton pulse is controlled well by varying the relative frequency. Moreover, we perform a spectral analysis on the asymmetric soliton pulse. The conclusion is given in Section 4.

2. Theoretical model and analytic solution

Nonlinear waves in single mode fiber (SMF) have been studied extensively, because of its important application in telecommunications system.[1–3] Most single-mode fiber is not truly single mode, because it usually involves two orthogonally polarized states. For real fibers, the two orthogonally polarized states usually are not degenerate but mixed randomly, which is called randomly birefringent optical fiber.[25] But when we discuss soliton dynamics under the case with relatively low-polarization mode dispersion, the group velocity difference between the two can be eliminated by a transformation.[25] Then, the propagation of two orthogonally polarized optical pulses can be described by Manakov equations.[26] Moreover, dispersion coefficient can be manipulated well in both theory and experiment.[25,27–32] Nonlinearity management was performed in Bose–Einstein condensates[33] and nonlinearity strength was manipulated well in optics using femtosecond pulses and layered Kerr media consisting of glass and air,[34] which provides possibilities to manipulate nonlinearity in Kerr optical fiber. Therefore, we introduce $\beta(z)$ and $g(z)$ to describe manipulations on the dispersion and nonlinear coefficients, respectively. Then the evolution of two orthogonally polarized optical pulses is written as:

$$\mathrm{i}\frac{\partial \varphi_1}{\partial z}+\beta(z)\frac{\partial^2 \varphi_1}{\partial t^2}+2g(z)[|\varphi_1|^2+|\varphi_2|^2]\varphi_1=0, \quad (1)$$

$$\mathrm{i}\frac{\partial \varphi_2}{\partial z}+\beta(z)\frac{\partial^2 \varphi_2}{\partial t^2}+2g(z)[|\varphi_1|^2+|\varphi_2|^2]\varphi_2=0, \quad (2)$$

where φ_1 and φ_2 are the slowly varying amplitudes of the two orthogonally polarized optical pulses. When $\beta(z)$ and $g(z)$ are constants, the theoretical model has been used to explain the experimental results for MI characters[35] and optical dark rogue waves in a randomly birefringent optical fiber.[36] The coupled partial differential equations can also be used to describe the dynamics of matter wave in quasi-one-dimensional two-component Bose-Einstein condensate,[37] the evolution of optical fields in fiber,[38] and even the vector financial system.[39]

We study the evolutions of weak modulations on generalized CWBs as $\varphi_{10}=s\mathrm{e}^{[\mathrm{i}4s^2z]}$, $\varphi_{20}=s\mathrm{e}^{[\mathrm{i}\Omega_\mathrm{r}t+\mathrm{i}(4s^2-\Omega_\mathrm{r}^2)z]}$, where s denotes the background amplitude and Ω_r denotes the relative frequency of the CWBs in the two components. Dispersion-decreasing fiber (DDF) is widely used in optical communications, due to its better transmission characteristics.[40] The propagation properties of optical solitons in the DDF have been studied.[41] In addition, exponential dispersion modulation has been realized in experiments.[42] Therefore we consider an exponential dispersion decreasing fiber system with $\beta(z)=a\mathrm{e}^{b(z-z_0)}$ in this paper,[43,44] where a, b, and z_0 are arbitrary real constants. The experiments show that the dispersion coefficient and nonlinearity coefficient can both be manipulated in some ways.[25,31–34] So we suppose $g(z)$ and $\beta(z)$ satisfy a definite constraint as $g(z)=\gamma^2\beta(z)$, where γ is arbitrary real constant. Under above containment relationship, the exact nonlinear localized wave's solutions of Eq. (1) and Eq. (2) can be obtained on the CWBs with the help of Darboux transformation and similar transformation.[21,45,46] The expressions of the solutions (φ_1 and φ_2) are presented in the Appendix A.

Based on the derived solutions, we find some different excitation patterns in this model, such as asymmetric W-shaped and M-shaped soliton pulses, dark–antidark (DAD) and antidark–dark (ADD) soliton pulse pair, symmetric W-shaped and M-shaped soliton pulse. To our knowledge, solitons are usually obtained from localized pulses.[19] However, the dynamical behaviors of soliton pulse excitation here are different, which shows that soliton pulses are generated from a weak modulation on continuous wave background.

In order to provide reference to experimental research, we transform the dimensionless parameters to experimental parameters by the parameters of a highly nonlinear fiber (OFS Speciality Fiber) with dispersion $\beta=-8.85\times10^{-28}$ s^2·m^{-1} and nonlinear $g=0.01$ W^{-1}·m^{-1}, as the ones in real experiment.[1] Under above parameters and input power $P_0=0.4$ W, the dimensional distance ξ (in unit m), time τ (in unit ps) and frequency ω (in unit THz) are related to the normalized parameters by $\xi=z\ L_\mathrm{NL}$ (m) , $\tau=t\ t_0$ (in unit ps) and $\omega=\Omega\ \omega_0$ (in unit THz) , where the characteristic length is $L_\mathrm{NL}=(g\ P_0)^{-1}=250$ m, times scale $t_0=(|\beta\ |L_\mathrm{NL})^{1/2}=0.47$ ps and frequency scale $\omega_0=(|\beta|\ L_\mathrm{NL})^{-1/2}=2.13$ THz. All following discussions are made with these parameter settings.

3. Asymmetric soliton pulse and asymmetric discontinuous spectrum

3.1. Asymmetric soliton pulse generated from a weak modulation on continuous wave background

We show the dynamical process in Fig. 1, for which one weak modulation signal on the CWBs evolves to be a stable soliton pulse in exponential dispersion decreasing fiber. It is shown that the peak (valley) of soliton pulse increases (decreases) firstly and then decreases (increases) along propagation direction.

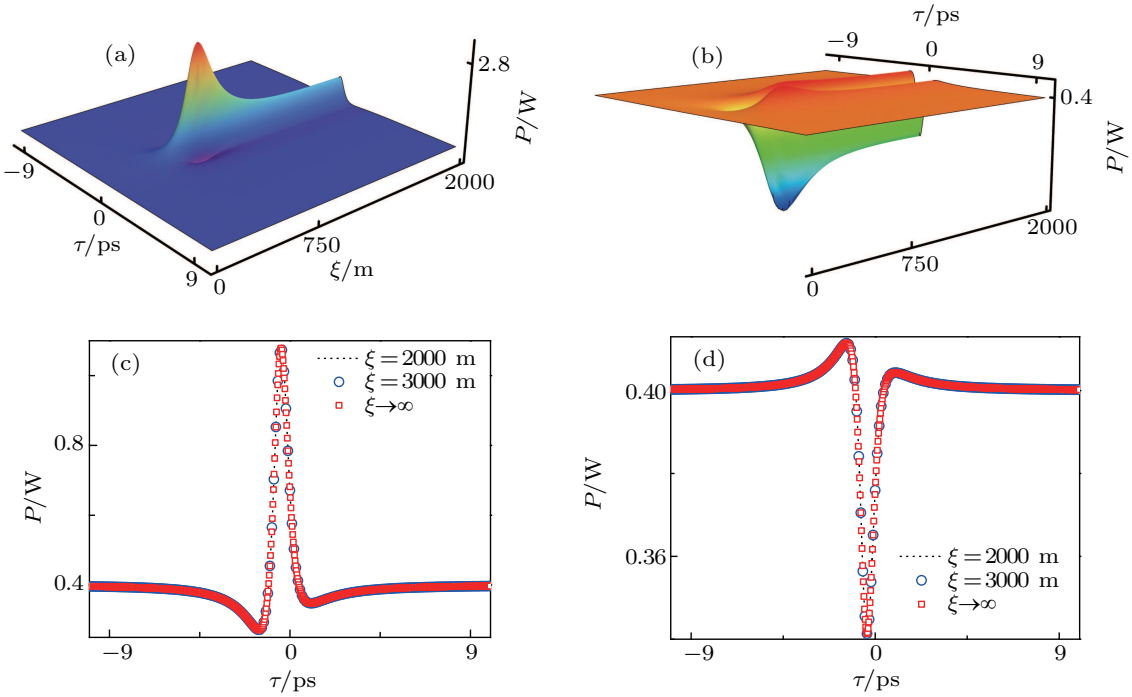


Fig. 1. (color online) The evolution of signal in two components corresponding to the process that one weak modulation signal evolves into asymmetric W-shaped soliton pulse and M-shaped soliton pulse (a) for $|\varphi_1|$ with $\omega_r = 0.85$ THz and (b) for $|\varphi_2|$ with $\omega_r = 10.65$ THz. The profile of signal at $\xi = 2000$ m, $\xi = 3000$ m, and $\xi \longrightarrow \infty$ ((c) for $|\varphi_1|$ with $\omega_r = 0.85$ THz and (d) for $|\varphi_2|$ with $\omega_r = 10.65$ THz). The other parameters are $a = 1$, $b = -1$, $s = 1$, $\gamma = 0.5$, and $\xi_0 = 750$ m.

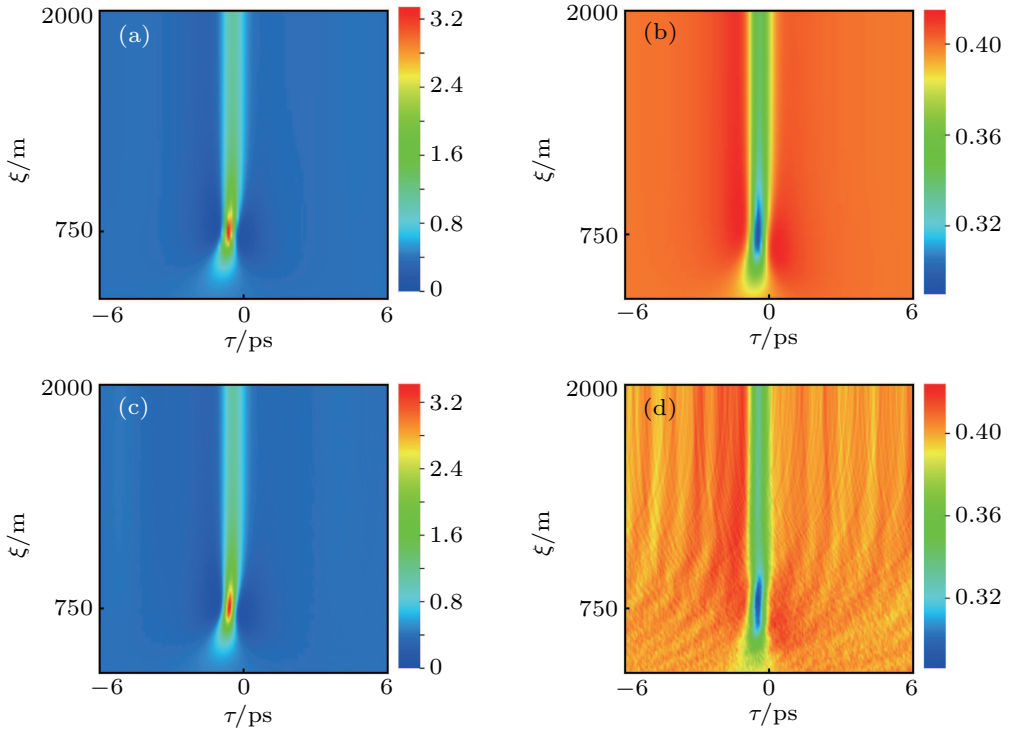


Fig. 2. (color online) The numerical simulation of the dynamics evolution process from an initial data given by the exact solution at $\xi = 375$ m (a) for $|\varphi_1|^2$ and (b) for $|\varphi_2|^2$. The numerical simulation corresponding to panels (a) and (b) with small noise. The initial excitation condition is given by the exact solution at $\xi = 375$ m by multiplying a factor $(1 + 0.01\text{Random}[-1, 1])$. The parameters are the same as those in Fig. 1.

However, after a certain distance, their changing rates tend to zero, namely, the profiles of soliton pulse are kept well. We can see the stable soliton pulses in two components are different. In order to present it more clearly, we demonstrate the profile of the soliton pulse at different distances in Fig. 1(c) for component φ_1 and Fig. 1(d) for component φ_2, based on analysis of distribution function. Moreover, the soliton pulses have asymmetry characters. In component φ_1, soliton pulse admits a W-shaped profile, which is similar to the ones obtained in Sasa-Satsuma equation[47] and coupled defocusing

Hirota equation.[48] But the two valleys here are asymmetric (see Fig. 1(c)), in contrast to symmetric cases. Therefore, it is named as "asymmetric W-shaped soliton pulse". Similarly, the soliton pulse in component φ_2 is named as "asymmetric M-shaped soliton pulse" (Fig. 1(d)). The asymmetric soliton pulses we obtained are stable, and the profile of soliton pulse is almost invariable after a certain transmission distance (see Fig. 1(c) and Fig. 1(d)). The dashed line, dot and square point express the profiles of analytic result at $\xi = 2000$ m, $\xi = 3000$ m, and $\xi \to \infty$ respectively.

In order to prove the feasibility of process for asymmetric soliton pulse generation, we numerically test Eq. (1) and (2) from an exact initial signal at certain locations for which the signals are weak by adopting the split-step Fourier method. To demonstrate the dynamical process clearly, we show the numerical results for $|\varphi_1|^2$ in Fig. 2(a) and $|\varphi_2|^2$ in Fig. 2(b). It is shown that the numerical results are in good agreement with the analytical results, even with numerical deviations. Considering the actual experiment, the initial condition cannot be given exactly and there are always some deviations in real experiments. Therefore, we test the stability of the generated asymmetric soliton pulse by adding white noise 0.01 Random $(\chi)(\chi \in [-1,1])$. The results indicate that they are robust against small noise or perturbation (see Fig. 2(c) for $|\varphi_1|^2$ and Fig. 2(d) for $|\varphi_2|^2$). This suggests that the exact process might be realized in experiments.

Then, what about the mechanism for asymmetric soliton pulse generated from a weak modulation. It is well known that MI can be used to explain the dynamics of different localized nonlinear waves.[49] The standard linear instability analysis is performed on CWBs ($\varphi_{10} = s\,\mathrm{e}^{\mathrm{i}[4s^2(1-\beta)]}$ and $\varphi_{20} = s\,\mathrm{e}^{\mathrm{i}[(4s^2-\Omega_\mathrm{r}^2)(1-\beta)+\Omega_\mathrm{r} t]}$). The weak perturbation with arbitrary Fourier modes are added on the CWBs, $\varphi_1 = \varphi_{10}\left\{1 + f_+\,\mathrm{e}^{[\mathrm{i}\Omega'(t-\Omega z)]} + f_-\,\mathrm{e}^{[-\mathrm{i}\Omega'(t-\Omega z)]}\right\}$ and $\varphi_2 = \varphi_{20}\left\{1 + g_+\,\mathrm{e}^{[\mathrm{i}\Omega'(t-\Omega z)]} + g_-\,\mathrm{e}^{[-\mathrm{i}\Omega'(t-\Omega z)]}\right\}$ (f_+, f_-, g_+, and g_- are small amplitudes of the Fourier modes). Substituting them to Eq. (1) and Eq. (2) and linearizing the equations, one can get the following dispersion relation:

$$\Omega^4 - 4\Omega^3\beta\Omega_\mathrm{r} + 4\Omega(\Omega'^2 - 4)\beta^3\Omega_\mathrm{r} - 2\Omega^2\beta^2(\Omega'^2 - 2\Omega_\mathrm{r}^2 - 4) + \beta^4(\Omega'^4 + 16\Omega_\mathrm{r}^2 - 8\Omega'^2 - 4\Omega_\mathrm{r}^2\Omega'^2) = 0. \quad (3)$$

We demonstrate the growth rate $\mathrm{Im}(\Omega)$ on the perturbation frequency ω' vs propagation distance ξ with $\omega_\mathrm{r} = 2.56$ THz in Fig. 3. We can see that the gain $\mathrm{Im}(\Omega)$ rapidly approaches zero when $\xi > 750$ m, namely the solution is transformed from MI regime to modulation stability (MS) regime. This can be used to understand the above dynamical process that the signal grows into a stable asymmetric soliton pulse gradually behind 750 m (see Fig. 1).

Interestingly, the profile of asymmetric soliton pulse can be varied through changing some physical parameters. Next, we discuss how to control the soliton pulse profile in the exponential dispersion decreasing fiber.

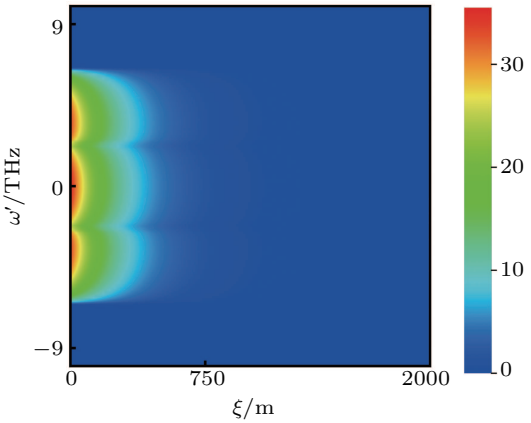


Fig. 3. (color online) MI gain distributed on propagation distance ξ and perturbation frequency ω' in exponential dispersion-managed fibre. The parameters are $a = 1$, $b = -1$, $s = 1$, $\gamma = 1$, and $\xi_0 = 750$ m.

3.2. State conversion and asymmetric degree

We define a symmetric degree to characterize the asymmetric property of the soliton pulse accurately under two different situations. For W-shaped soliton pulse, the symmetric degree is defined as $\Theta(\Omega_\mathrm{r}) = (1 - |\varphi_{1,2}|^2_{\min 1})/(1 - |\varphi_{1,2}|^2_{min2})$, which stands for the ratio of depths of two valleys. For M-shaped soliton pulse, the symmetric degree is $\Theta(\Omega_\mathrm{r}) = (|\varphi_{1,2}|^2_{\max 1} - 1)/(|\varphi_{1,2}|^2_{\max 2} - 1)$, which stands for the ratio of heights of two humps. We choose the smaller value to be numerator, to set $0 \le \Theta(\Omega_\mathrm{r}) \le 1$. The symmetric degree versus ω_r in two components is presented in Fig. 4 (Fig. 4(a) for component φ_2 and Fig. 4(b) for component φ_1). Taking component φ_2 as an example, the symmetric degree decreases firstly and then increases with the increase of ω_r, for which the minimum value emerges at $\omega_\mathrm{r} = 2.13$ THz. Based on three critical points ($\omega_\mathrm{r} = 0$ THz, $\omega_\mathrm{r} = 2.13$ THz, and $\omega_\mathrm{r} \to \infty$), the soliton pulse states are classified into five cases (see Fig. 4(a)) as follows:

(i) When $\omega_\mathrm{r} = 0$ THz, the symmetric degree will be $\Theta(\omega_\mathrm{r}) = 1$ and the soliton pulse is "symmetry W-shaped soliton pulse". Similar soliton state was obtained in Sasa-Satsuma equation[47] and coupled defocusing Hirota equation.[48]

(ii) When 0 THz$< \omega_\mathrm{r} <$ 2.13 THz, the $\Theta(\omega_\mathrm{r})$ decreases quickly and the soliton pulse state is "asymmetry W-shaped soliton pulse", which is different from the former research.[47,48]

(iii) When $\omega_\mathrm{r} = 2.13$ THz, the $\Theta(\omega_\mathrm{r})$ reaches a minimum value and the soliton pulse state is "AD-D pair", which is similar to the result in Ref. [50].

(iv) When $\omega_\mathrm{r} > 2.13$ THz, the $\Theta(\omega_\mathrm{r})$ increases with ω_r . It is interesting that the soliton pulse state shows inversion phenomenon, which possesses one valley and two crests and is named "asymmetry M-shaped soliton pulse".

(v) When $\omega_\mathrm{r} \to \infty$, the $\Theta(\omega_\mathrm{r})$ slowly approaches 1 and the soliton pulse state will be converted into "symmetry M-shaped

soliton pulse".

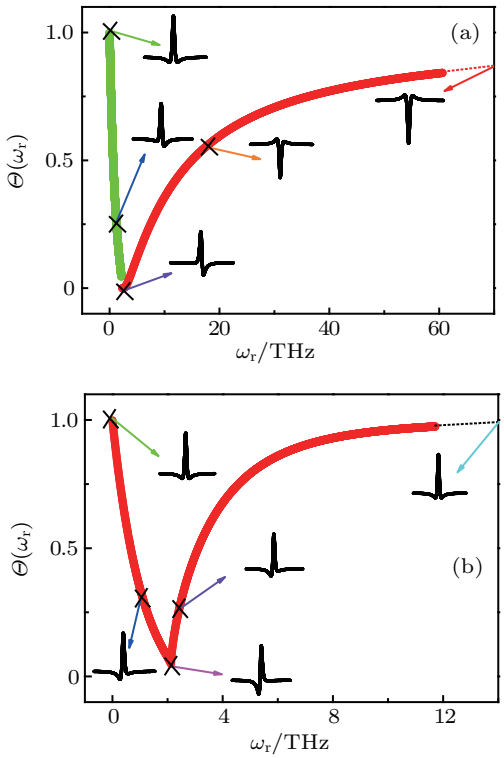


Fig. 4. (color online) The symmetric degree $\Theta(\omega_r)$ changes with ω_r in two components: (a) for component φ_2, (b) for component φ_1. The parameters are $a=1$, $b=-1$, $s=1$, $\gamma=0.5$, and $\xi_0=750$ m.

The state conversions in the component φ_1 are shown in Fig. 4(b). When $\omega_r < 2.13$ THz, the situation is similar to the component φ_2, which can achieve state conversion from "symmetric W-shaped soliton pulse" to "asymmetric W-shaped soliton pulse". But for $\omega_r \geq 2.13$ THz, the state in component φ_1 is different from the component φ_2. Explicitly, for $\omega_r = 2.13$ THz, the soliton pulse state in φ_1 is "D-AD pair", which is different from the "AD-D pair" in φ_2. For $\omega_r > 2.13$ THz, the soliton pulse in φ_1 evolves to "asymmetric W-shaped soliton pulse" and then "symmetric W-shaped soliton pulse" in contrast to the M-shaped soliton pulse in φ_2.

In this section, we demonstrate that asymmetric and symmetric soliton pulses can be controllably generated from a dispersion modulation. The dynamics of them are shown in temporal distribution. However, measuring the exact wave profiles in time domain can be problematic, but spectra measurement is a well developed technique which is supported by a multiplicity of devices used in experimental optics.[51,52] In the next section, we characterize the spectrum of the asymmetric soliton pulse.

3.3. Asymmetric discontinuous spectrum

The spectrum analysis is carried out through Fourier transformation,

$$F_{1,2}(\Omega,z) = \frac{1}{\sqrt{2\pi}}\int_{-\infty}^{+\infty}\varphi_{1,2}(t,z)\exp[\mathrm{i}\Omega t]\,\mathrm{d}t. \quad (4)$$

The solution can be written in the form of a constant background pulsing a signal. The Fourier transformation of constant background is infinity and thus it can be represented as $\delta(\Omega-\Omega_0)$, and then we can eliminate the δ function and obtain the spectrum of soliton pulse. We represent above spectrum intensity using a logarithmic density scale truncated at -40 dB relative to the maximum value. The corresponding spectrum density of soliton pulse in component φ_1 and φ_2 is

$$10\log_{10}\frac{|F_1(\omega,\xi)|^2}{|F_1(\omega,\xi)|^2_{\max}}\ (\mathrm{dB})$$

and

$$10\log_{10}\frac{|F_2(\omega'',\xi)|^2}{|F_2(\omega'',\xi)|^2_{\max}}\ (\mathrm{dB})$$

($\omega''=\omega+\omega_r$) respectively, as shown in the following Fig. 5(a) and Fig. 5(b).

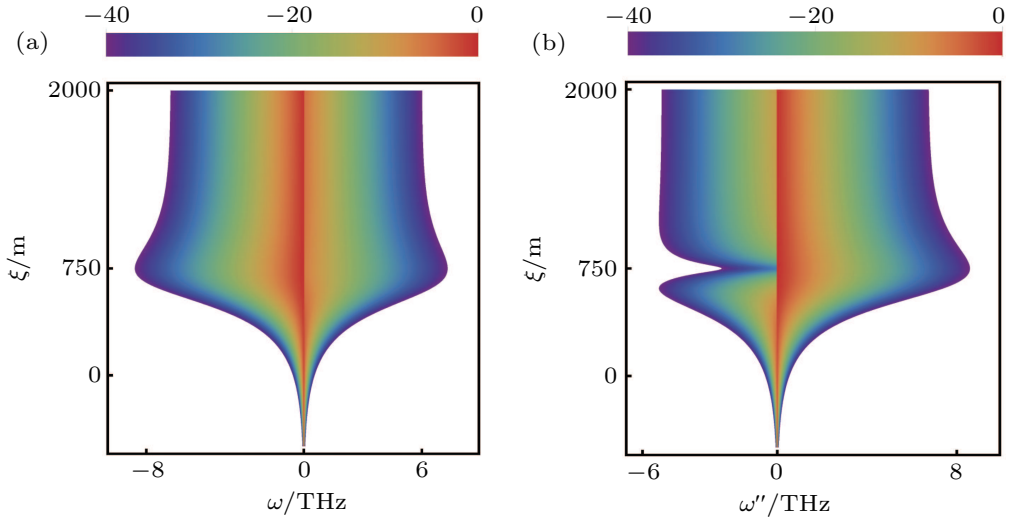


Fig. 5. (color online) (a) The spectrum intensity evolution of the soliton pulse in component φ_1. (b) The spectrum density evolution (where $\omega''=\omega+2.34$ THz) of the soliton pulse in component φ_2. The parameters are $\omega_r=2.34$ THz, $a=1$, $b=-1$, $s=1$, $\gamma=0.5$, and $\xi_0=750$ m.

In component φ_1, the spectral distribution is asymmetric on the two sides of background frequency. The spectrum density on the lower frequency (compared with background frequency) is much higher than the one on higher frequency. This result comes from the asymmetry of soliton pulse, which is different from the spectrum of soliton reported previously.[24] In component φ_2, the spectral distribution is still asymmetric, but the higher spectrum density is on the higher frequency. Moreover, it is seen that there are discontinuity points on the spectral distribution. Therefore, the spectrum is named as "asymmetric discontinuous spectrum". The degree of discontinuity achieves maximum at $\xi = 750$ m, then it decreases slowly with propagation distance and tends to a constant. The final degree of discontinuity is determined by the asymmetric property of soliton pulse.

4. Conclusion and discussion

In summary, we obtain a series of asymmetric and symmetric soliton pulses generated from a weak modulation in an exponential dispersion decreasing fiber. The quantitative relations between state transition (variation of symmetric degree) and relative frequency are summarized in Table 1. The numerical simulations indicate that the dynamical process is robust against weak noise or perturbation. Furthermore, the spectrum analysis indicates that the asymmetric soliton pulse admits "asymmetric discontinuous spectrum". The results provide another possible way to obtain asymmetric soliton pulses from weak modulations.

Table 1. Quantitative relations between the state conversion (variation of symmetric degree) and the relative frequency ω_r.

ω_r/THz	Soliton state of φ_1	Soliton state of φ_2	$\Theta(\omega_r)$
$\omega_r = 0$	symmetric W-shaped soliton pulse	symmetric W-shaped soliton pulse	$\Theta(\omega_r) = 1$
$0 < \omega_r < 2.13$	asymmetric W-shaped soliton pulse	asymmetric W-shaped soliton pulse	$0 < \Theta(\omega_r) < 1$
$\omega_r = 2.13$	D-AD soliton pulse pair	AD-D soliton pulse pair	$\Theta(\omega_r) \to 0$
$\omega_r > 2.13$	asymmetric W-shaped soliton pulse	asymmetric M-shaped soliton pulse	$0 < \Theta(\omega_r) < 1$
$\omega_r \to \infty$	symmetric W-shaped soliton pulse	symmetric M-shaped soliton pulse	$\Theta(\omega_r) \to 1$

Now, based on the dynamics formation process of asymmetric soliton pulse, we discuss the feasible experimental scheme and perform a numerical test. The formation process of dynamics is as follows. A weak perturbation on the continuous wave backgrounds rapidly grows into a high energy pulse under the modulational instability (MI) regimes, then decays slowly due to the inhibited MI which is caused by dispersion and nonlinear management, and finally evolves into a stable asymmetric soliton pulse corresponding to modulational stability (MS) regimes. The process of MI growth is consistent with the dynamic process which experimentally stimulates the dark rogue wave in Manakov system.[36] Moreover, the experiments show that both the dispersion and nonlinearity coefficient can be manipulated in some way.[33,34,42] We only need to inject two weak orthogonally polarized optical pulses into a randomly birefringent dispersion optical fiber in the same way as Ref. [36] and set the dominant frequency of optical pulses equal to the one of continuous wave background. The relative frequency of continuous wave backgrounds and other parameters in two components are set as shown in Fig. 1. Then, the optical pulses in two states will evolve into "asymmetric W-shaped and M-shaped soliton pulses" respectively after a certain transmission distance as shown in Fig. 1(c) and 1(d). The asymmetry of the soliton pulse is caused by the frequency difference of continuous wave backgrounds in two components. Following the above steps, we carried out a numerical test. The numerical results show that the "asymmetric W-shaped and M-shaped soliton pulses" can be obtained. The numerical results agree well with the analytical results, and even with numerical deviations (see Figs. 2(a) and 2(b)). Furthermore, we have tested the stability of the generated asymmetric soliton pulses with adding white noise 0.01 Random (χ) $(\chi \in [-1, 1])$. The results indicate that they are robust against small noise or perturbation (see Figs. 2(c) and 2(d)). This suggests that the exact process might be realized in experiments.

A dispersion manipulation on defocusing fiber demonstrated some striking dynamical behaviors[53] and CWB has been used widely to generate rogue wave and breather.[1,3] Recently, optical dark rogue wave has been observed in Manakov system.[36] Based on the developed phase and density manipulation techniques and dispersion manipulation experiment, we believe the results in this paper would be tested experimentally in the near future.

Appendix A: Expressions of the solutions φ_1 and φ_2

$$\varphi_1 = s\mathrm{e}^{\phi_1}\left[1 - \frac{\mathrm{i}6bb_1|A_2|^2A_3M_1M_3^*}{A_1(9s^2b^2|A_2|^2|M_1|^2 + 9s^2b^2A_3|M_2|^2 + |A_2|^2A_3|M_3|^2)}\right],$$

$$\varphi_2 = s\mathrm{e}^{\phi_2}\left[1 - \frac{\mathrm{i}6bb_1|A_2|^2A_3M_2M_3^*}{A_2(9s^2b^2|A_2|^2|M_1|^2 + 9s^2b^2A_3|M_2|^2 + |A_2|^2A_3|M_3|^2)}\right],$$

$$M_1(t,z) = -\frac{9\mathrm{i}}{A_1} - \frac{2\gamma^2 aA_1}{b}[\mathrm{e}^{b(z-z_0)} - 1] - 3\gamma t - 3,$$

$$M_2(t,z) = -\frac{9\mathrm{i}}{A_2} - \frac{2\gamma^2 aA_1}{b}[\mathrm{e}^{b(z-z_0)} - 1] - 3\gamma t - 3,$$

$$M_3(t,z) = 2\gamma^2 aA_1[\mathrm{e}^{b(z-z_0)} - 1] + 3b(1+\gamma t),$$

$$A_1 = a_1 - 3\mathrm{i}a_2 - \mathrm{i}b_1 - 3b_2 - \Omega_\mathrm{r},$$
$$A_2 = a_1 - 3\mathrm{i}a_2 - \mathrm{i}b_1 - 3b_2 + 2\Omega_\mathrm{r},$$

$$A_3 = a_1^2 + b_1^2 + 9a_2^2 + 9b_2^2 + 6a_2b_1 + 6b_2\Omega_\mathrm{r} + \Omega_\mathrm{r}^2 - 2a_1(3b_2 + \Omega_\mathrm{r}),$$

$$\phi_1 = \frac{\mathrm{i}4s^2\gamma^2 a}{b}[\mathrm{e}^{b(z-z_0)} - 1],$$
$$\phi_2 = -\frac{\mathrm{i}\gamma^2 a(\Omega_\mathrm{r}^2 - 4s^2)}{b}[\mathrm{e}^{b(z-z_0)} - 1] + \mathrm{i}\gamma\Omega_\mathrm{r} t,$$

$$a_1 = \mathrm{Re}[\lambda], \quad b_1 = \mathrm{Im}[\lambda], \quad a_2 = \mathrm{Re}[\theta], \quad b_2 = \mathrm{Im}[\theta],$$
$$\lambda = \frac{\sqrt{\Omega_\mathrm{r}^6 - 4\Omega_\mathrm{r}^2[5\Omega_\mathrm{r}^2 s^2 + 2s^4 - 2\sqrt{-s^2(\Omega_\mathrm{r}^2 - s^2)^3}]} - \Omega_\mathrm{r}^3}{2\Omega_\mathrm{r}^2},$$

$$\theta = \frac{\mathrm{i}[2\lambda^3 + 3\Omega_\mathrm{r}\lambda^2 + (18s^2 - 3\Omega_\mathrm{r}^2)\lambda] - \mathrm{i}(2\Omega_\mathrm{r}^3 - 9\Omega_\mathrm{r}s^2)}{2(3\Omega_\mathrm{r}^2 + 3\lambda^2 + 3\Omega_\mathrm{r}\lambda + 18s^2)}.$$

References

[1] Kibler B, Fatome J, Finot C, Millot G, Dias F, Genty G, Akhmediev N and Dudley J M 2010 *Nat. Phys.* **6** 790
[2] Dudley J M, Genty G, Dias F, Kibler B and Akhmediev N 2009 *Opt. Express* **17** 21497
[3] Kibler B, Fatome J, Finot C, Millot G, Genty G, Wetzel B and Dudley J M 2012 *Sci. Rep.* **2** 463
[4] Zhong W P, Xie R H, Beli M, Petrovi N and Chen G 2008 *Phys. Rev. A* **78** 023821
[5] Wang Y Y, Dai C Q and Wang X G 2014 *Nonlinear Dyn.* **77** 1323
[6] Li Z D, Wu X, Li Q Y and He P B 2015 *Chin. Phys. B* **25** 010507
[7] Liu Y K and Li B 2017 *Chinese Physics Letters* **34** 010202
[8] Dai C Q, Chen R P, Wang Y Y and Fan Y 2017 *Nonlinear Dyn.* **87** 1675
[9] Yang J K 1997 *Physica D* **108** 92
[10] Kanna T and Lakshmanan M 2001 *Phys. Rev. Lett.* **86** 5043
[11] He J S, Mei J and Li Y S 2007 *Chin. Phys. Lett.* **24** 2157
[12] Dai C Q, Fan Y, Zhou G Q, Zheng J and Chen L 2016 *Nonlinear Dyn.* **86** 999
[13] Guo B L and Ling L M 2011 *Chin. Phys. Lett.* **28** 110202
[14] Baronio F, Degasperis A, Conforti M and Wabnitz S 2012 *Phys. Rev. Lett.* **109** 044102
[15] Chen S, Song L Y 2013 *Phys. Rev. E* **87** 032910
[16] Zhao L C and Liu J 2013 *Phys. Rev. E* **87** 013201
[17] Wang Y Y, Dai C Q, Zhou G Q, Fan Y and Chen L 2017 *Nonlinear Dyn.* **87** 67
[18] Liu C, Yang Z Y, Zhao L C and Yang W L 2014 *Phys. Rev. A* **89** 055803
[19] Kivshar Y and Agrawal G 2003 *Optical Solitons: From Fibers to Photonic Crystals* (London: Academic)
[20] Akhmediev N, Ankiewicz A and Soto-Crespo J M 2009 *Phys. Rev. E* **80** 026601
[21] Guo B L, Ling L M and Liu Q P 2012 *Phys. Rev. E* **85** 026607
[22] Baronio F, Conforti M, Degasperis A, Lombardo S, Onorato M and Wabnitz S 2014 *Phys. Rev. Lett.* **113** 034101
[23] Dai C Q, Zhou G Q and Zhang J F 2012 *Phys. Rev. E.* **85** 016603
[24] Duan L, Yang Z Y, Zhao L C and Yang W L 2016 *J. Mod. Opt.* **63** 1397
[25] Agrawal G 2007 *Nonlinear Fiber Optics*, 4th edn. (New York: Academic)
[26] Manakov S V 1974 *Soviet Physics-JETP* **38** 248
[27] Smith N J, Doran N J, Forysiak W and Knox F M 1997 *J. Lightwave Technol.* **15** 1808
[28] Porsezian K, Hasegawa A, Serkin V N, Belyaeva T L and Ganapathy R 2007 *Phys. Lett. A* **361** 504
[29] Rajan M M, Hakkim J, Mahalingam A and Uthayakumar A 2013 *Eur. Phys. J. D* **67** 150
[30] Hao R, Li L, Li Z, Xue W and Zhou G 2004 *Opt. Commun.* **236** 79
[31] Chang C C, Sardesai H P and Weiner A M 1998 *Opt. Lett.* **23** 283
[32] Yamamoto T and Nakazawa M 2001 *Opt. Lett.* **26** 647
[33] Pelinovsky D E, Kevrekidis P G and Frantzeskakis D J 2003 *Phys. Rev. Lett.* **91** 240201
[34] Centurion M, Porter M A, Kevrekidis P G and Psaltis D 2006 *Phys. Rev. Lett.* **97** 033903
[35] Frisquet B, Kibler B, Fatome J, Morin P, Baronio F, Conforti M, Millot G and Wabnitz S 2015 *Phys. Rev. A* **92** 053854
[36] Frisquet B, Kibler B, Morin P, Baronio F, Conforti M, Millot G and Wabnitz S 2016 *Sci. Rep.* **6** 20785
[37] Hamner C, Chang J J, Engels P and Hoefer M A 2011 *Phys. Rev. Lett.* **106** 065302
[38] Tang D Y, Zhang H, Zhao L M and Wu X 2008 *Phys. Rev. Lett.* **101** 153904
[39] Yan Z Y 2011 *Phys. Lett. A* **375** 4274
[40] Jia R X, Wang Y C, Liu W J and Lei M 2013 *J. Mod. Opt.* **60** 1993
[41] Liu W J, Zhang Y, Pang L, Yan H, Ma G and Lei M 2016 *Nonlinear Dyn.* **86** 1069
[42] Bogatyrev V A, Bubnov M M, Dianov E M, Kurkov A S, Mamyshev P V, Prokhorov A M and Chernikov S V 1991 *J. Lightwave Technol.* **9** 561
[43] Hao R Y, Li L, Li Z and Zhou G S 2004 *Phys. Rev. E* **70** 066603
[44] Wang Y Y, Dai C Q, Zhou G Q, Fan Y and Chen L 2017 *Nonlinear Dyn.* **87** 67
[45] Xu T, Wang D H, Li M and Liang H 2014 *Phys. Scr.* **89** 075207
[46] Yang Z Y, Zhao L C, Zhang T, Feng X Q and Yue R H 2011 *Phys. Rev. E* **83** 066602
[47] Zhao L C, Li S C and Ling L M 2014 *Phys. Rev. E* **89** 023210
[48] Huang X 2016 *Phys. Lett. A* **380** 2136
[49] Zhao L C and Ling L M 2016 *J. Opt. Soc. Am. B* **33** 850
[50] Zhao L C, Yang Z Y and Ling L M 2014 *J. Phys. Soc. Jpn.* **83** 104401
[51] Workman J and Art Springsteen J 1998 *Applied Spectroscopy* (London: Academic Press)
[52] Hollas J M 2004 *Modern Spectroscopy*, 4th edn. (Chichester: John Wiley & Sons Ltd)
[53] Conforti M, Mussot A, Kudlinski A, Nodari S R, Dujardin G, De Biévre S and Trillo S 2016 *Phys. Rev. Lett.* **117** 013901